STINFO COPY

AFRL-HE-WP-TP-2007-0002

Stochastic Resonance Investigation of Object Detection in Images

Daniel W. Repperger
Alan R. Pinkus
Warfighter Interface Division
Battlespace Visualization Branch
Wright-Patterson AFB OH 45433-7022

Julie A. Skipper
Christina D. Schrider
Wright State University
Department of Biomedical
Human Factors and Industrial Engineering
Dayton OH 45435

December 2006

Interim Report for the period November 2006 to December 2006

Air Force Research Laboratory
Human Effectiveness Directorate
Warfighter Interface Division
Battlespace Visualization Branch
Wright-Patterson AFB OH 45433

REPORT DOCUMENTATION PAGE

Form Approved
OMB No. 0704-0188

1. REPORT DATE *(DD-MM-YYYY)*	2. REPORT TYPE	3. DATES COVERED *(From - To)*
1 Dec 2006	Interim	November 2006 – December 2006

4. TITLE AND SUBTITLE
Stochastic Resonance Investigation of Object detection in images

5a. CONTRACT NUMBER
In-House

5b. GRANT NUMBER

5c. PROGRAM ELEMENT NUMBER
61102F

6. AUTHOR(S)
Daniel W. Repperger*
Alan R. Pinkus*
Julie A. Skipper**
Christina D. Schrider**

5d. PROJECT NUMBER
2313

5e. TASK NUMBER
HC

5f. WORK UNIT NUMBER
54

7. PERFORMING ORGANIZATION NAME(S) AND ADDRESS(ES)
Wright State University Department of Biomedical**
Human Factors and Industrial Engineering
Dayton OH 45435

8. PERFORMING ORGANIZATION REPORT NUMBER

9. SPONSORING/MONITORING AGENCY NAME(S) AND ADDRESS(ES)
Air Force Materiel Command*
Air Force Research Laboratory
Human Effectiveness Directorate
Warfighter Interface Division
Battlespace Visualization Branch
Wright Patterson AFB OH 45433-7022

10. SPONSOR/MONITOR'S ACRONYM(S)
AFRL/HECP

11. SPONSORING/MONITORING AGENCY REPORT NUMBER
AFRL-HE-WP-TP-2007-0002

12. DISTRIBUTION AVAILABILITY STATEMENT
Approved for public release; distribution is unlimited.

13. SUPPLEMENTARY NOTES
AFRL/PA Cleared 1/12/2007, AFRL/WS-07-0075.

14. ABSTRACT
Object detection in images was conducted using a nonlinear means of improving signal to noise ratio termed “stochastic resonance” (SR). In a recent United States Paten application, it was shown that arbitrarily large signal to noise ratio gains could be realized when a signal detection problem is cast within the context of a SR filter. Signal-to-noise ratio measures were investigated. For a binary object recognition task (friendly versus hostile), the method was implemented by perturbing the recognition algorithm and subsequently thresholding via a computer simulation.

15. SUBJECT TERMS
Stochastic resonance, nnonlinear dynamics, object identification, signal-to-noise ratio amplification

16. SECURITY CLASSIFICATION OF: Unclassified			17. LIMITATION OF ABSTRACT	18. NUMBER OF PAGES	19a. NAME OF RESPONSIBLE PERSON
a. REPORT	b. ABSTRACT	c. THIS PAGE			Daniel W. Repperger
U	U	U	SAR	14	19b. TELEPONE NUMBER (*Include area code*)

Stochastic resonance investigation of object detection in images

Daniel W. Repperger*[1], Alan R. Pinkus[1], Julie A. Skipper[2], Christina D. Schrider[2]

[1]Air Force Research Laboratory, AFRL/HEC, Wright-Patterson AFB, Ohio, 45433 USA;
[2]Wright State Univ. Dept. of Biomedical, Human Factors and Industrial Eng. Dayton, Ohio 45435

ABSTRACT

Object detection in images was conducted using a nonlinear means of improving signal to noise ratio termed "stochastic resonance" (SR). In a recent United States patent application, it was shown that arbitrarily large signal to noise ratio gains could be realized when a signal detection problem is cast within the context of a SR filter. Signal-to-noise ratio measures were investigated. For a binary object recognition task (friendly versus hostile), the method was implemented by perturbing the recognition algorithm and subsequently thresholding via a computer simulation. To fairly test the efficacy of the proposed algorithm, a unique database of images has been constructed by modifying two sample library objects by adjusting their brightness, contrast and relative size via commercial software to gradually compromise their saliency to identification. The key to the use of the SR method is to produce a small perturbation in the identification algorithm and then to threshold the results, thus improving the overall system's ability to discern objects. A background discussion of the SR method is presented. A standard test is proposed in which object identification algorithms could be fairly compared against each other with respect to their relative performance.

Keywords: Stochastic Resonance, nonlinear dynamics, object identification, signal-to-noise ratio amplification.

1. INTRODUCTION

Certain properties of nonlinear systems may be beneficial in improving sensitivity to the identification of objects in a compromised image. The nonlinear effect known as stochastic resonance has been known since 1981, Ref. 1, when it provided an early explanation for the calculation of the unusual periods of the earth's ice age. This resulted when the empirical results mismatched the theoretical predictions by an order of magnitude. To describe the SR effect, it applies when a weak, subliminal signal is masked in noise or other background interference and the goal is to correctly detect the state of the concealed signal during the time it is in a high state. The SR effect has been widely studied with biological signals (Ref. 2 and Ref. 3), in tactile sensation or haptics (Ref. 4 and Ref. 5), and in electronic circuits (Ref.6). This nonlinear phenomenon has produced some interest in detectability investigations (Ref. 7 and Ref. 8). It has also shown improvement or amplification of signal-to noise ratios (Ref. 9-13). A resonance in the amount of mutual information transferred across an information channel can be demonstrated (Ref. 14-22). Such a methodology has applicability to enhancing images (Ref. 23-24) and for special medical applications (Ref. 25). In Ref. 26, SR techniques have been generalized to include concurrent optimization with respect to parameter selection. In Ref. 27, multivariable problems are considered. The goal in this work is to explore and better understand the underlying mechanism of why SR works and apply such a procedure for improving identification of objects in images. We now describe two means of interpreting the SR effect as it occurs in Physics. From these two concepts a new class of mathematical means to synthesizing the SR outcome is discussed. A generalization to SR filters is provided. Examples are first worked on a signal processing application and then translated into the object recognition problem in images.

* d.repperger@ieee.org; phone 1-937-255-8765; fax 1-937-255-8752

2. STOCHASTIC RESONANCE IN PHYSICS - EXAMPLE 1 – A THRESHOLD VIEWPOINT

The pervasive appearance of SR in biological systems can be easily understood by examining a simple threshold model of a biological process. In Fig. 1, the top diagram displays a subliminal signal *S(t)* below a threshold of *T* units. If *S(t)* does not pierce through the threshold *T*, it is not detected, even though it is in its high state. The signal *S(t)* may be either in the high state (value = $h < T$) or in the low state (value =0). It is clear that there is a 100% chance of incorrectly identifying the high state of *S(t)* because it is always subtheshold. However, in all biological systems, there are various sources and levels of noise. In the middle diagram in Fig. 1, a zero mean noise of low variance is now added to *S(t)*. It is seen that on certain occasions, the sum of signals of *S(t)* + noise will exceed the threshold *T* and be detected, especially when *S(t)* is in the high state. Thus, from a detection point of view, the number of missed negatives (when

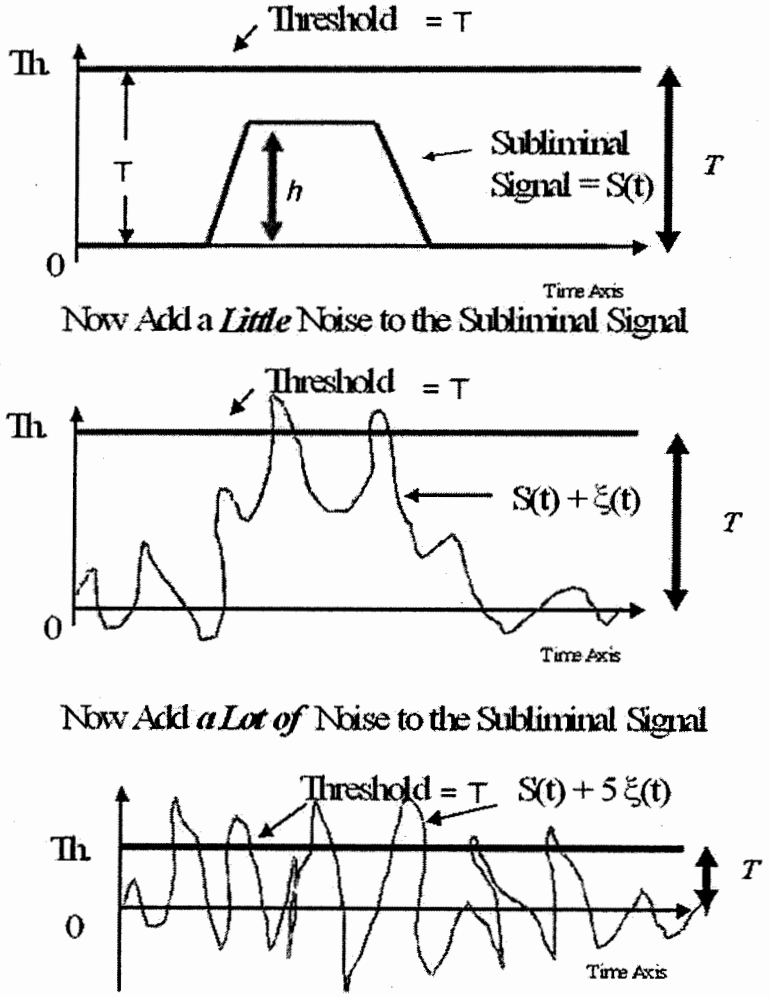

Fig. 1. A threshold representation of the SR effect

S(t) is high) is reduced and the noise has been helpful. The noise will have limiting advantage, however. In the bottom diagram of Fig 1., the noise has now been increased in variance and, accordingly, the signal *S(t)* + higher noise power produces false positives as well as reduces the number of missed negatives when it was in the high state. A summary of these results is displayed in Fig. 2. Herein the y axis is the probability of *correctly* detecting *S(t)* in the high state. At the origin, for the x-axis (noise power = 0), this probability is near zero. As the zero mean noise variance increases (moving to the right on the x axis), the SR curve rises because the number of missed negatives of detection rapidly

decreases (with some small number of increases in false positives). The curve in Fig. 2 reaches a maximum at an optimum amount of noise power. To the right of the optimum noise point, the noise is still increasing in power;

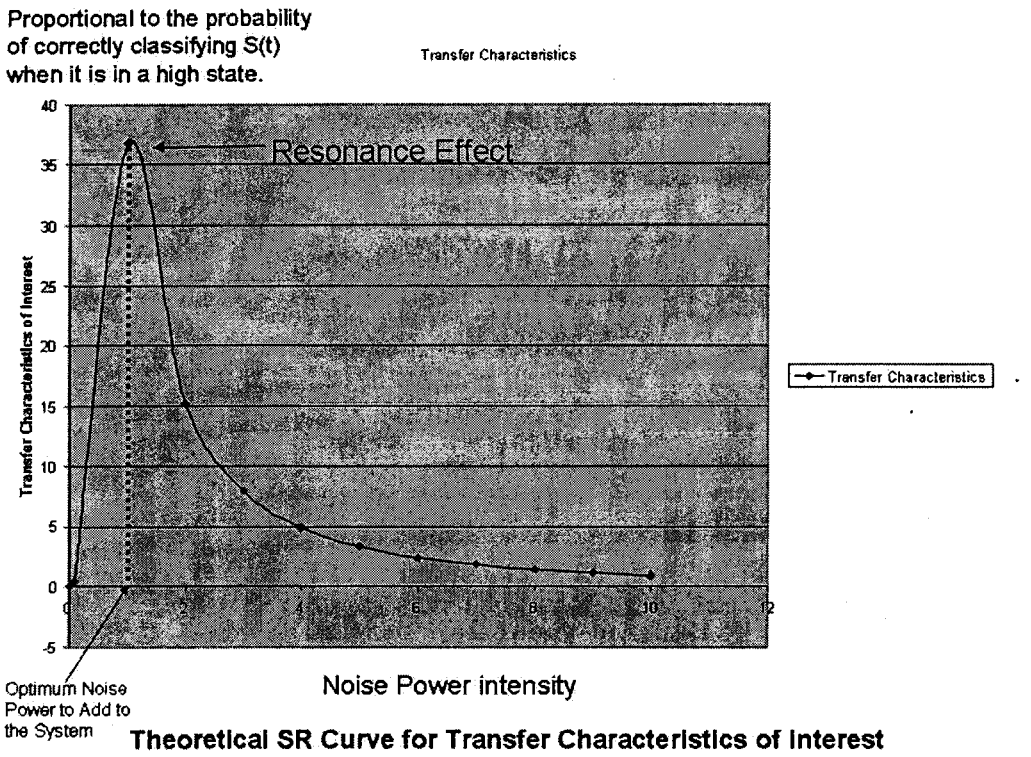

Fig. 2 – The stochastic resonance curve

however the gain realized by reducing the missed negatives is outweighed by the increasing number of false positives. Eventually, as the noise becomes very large, the system returns to the state where there is little benefit in adding the noise. This is called a SR curve because noise is added (stochastic) and a resonance effect is observed, as in Fig. 2. A second type of SR effect can be observed in a different Physics example involving a bipotential well.

3. STOCHASTIC RESONANCE IN PHYSICS - EXAMPLE 2 – A BIPOTENTIAL WELL

A second way to interpret the SR effect can be seen in the early work in physics with an example called a bipotential well. Fig. 3 portrays such a rendering. There is a direct analogy between Fig. 3 and Fig. 1. In Fig. 3 the ball is either in the left potential well (low state) or the right potential well (high state). In this case, the ball does not have enough potential energy (max $|S(t)| = h < T$) so it is difficult to make the ball switch states when it should be in the right potential well ($S(t)$ is in the high state). The addition of noise to the signal $S(t)$ in Fig 3 will accomplish the same goals as described previously with Figs. 1-2. Thus the bi-potential well is another means of viewing the SR effect, with analogy to the threshold model in Fig. 1. The bipotential well example, however, allows a mathematical framework to derive the dynamical equations of interest.

4. MATHEMATICAL FORMULATION OF THE SR CONCEPT

With reference to Fig. 3, the equations of motion of the dynamical system can be derived which leads to a better understanding, in a mathematical way, of why the SR effect works. In Fig. 3, three physical equilibrium points are observed at ($x = 0$, unstable, $x = \pm 1$ both stable) and denoted at the bottom of the figure. A quartic expression for the potential function $V(x)$ can be derived to fit the shape of Fig. 3 as follows:

$$V(x) = -(a^2)\,x^2/2 + x^4/4 \tag{1}$$

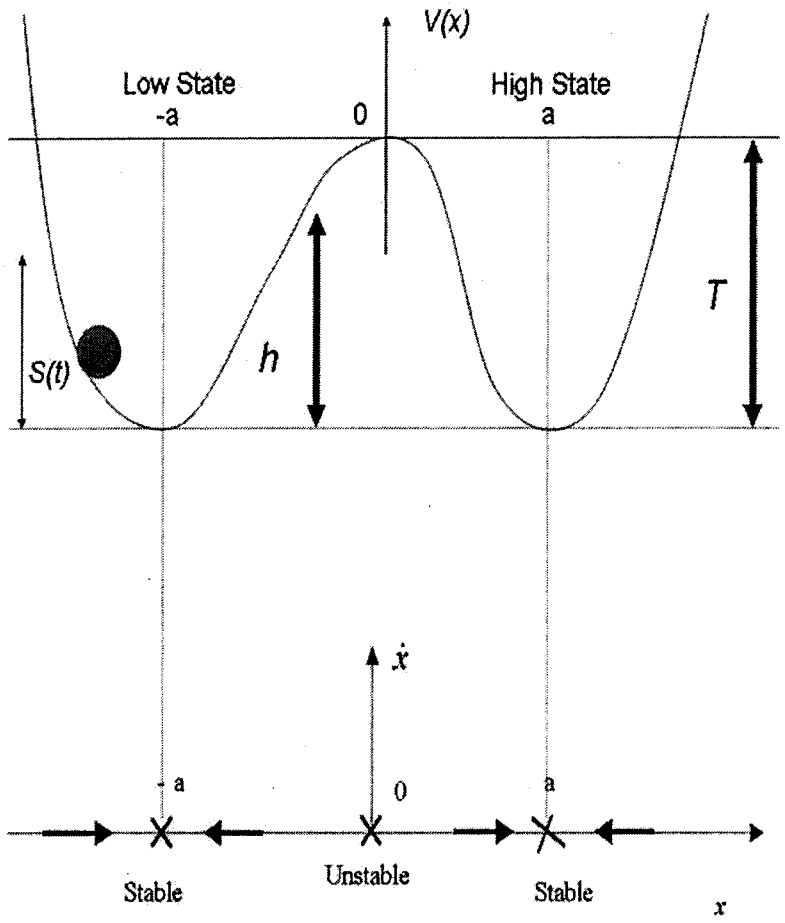

Fig. 3 – A second physics example to explain the SR effect

To derive the equations of motion, the forces acting on the ball can be shown to be related to the spatial change of the potential energy and external disturbances $S(t)$ with noise $\xi(t)$ resulting in the following equation:

$$\dot{x} = \frac{-\partial V(x)}{\partial x} + S(t) + \xi(t) \tag{2}$$

Substituting equation (1) into equation (2) gives rise to the following nonlinear differential equation describing the SR effect:

$$\dot{x} = -x(x^2 - a^2) + S(t) + \xi(t) \tag{3}$$

The homogenous form of this equation and its equilibrium points are most interesting and occur when:

$$\dot{x} = -x(x^2 - a^2) = 0, \tag{4}$$

which yields the three equilibrium points ($x = 0$, unstable), ($x = \pm a$, both stable) as shown in Fig. 3. Examining the physical and mathematical equilibrium points in Fig. 3 shows the concurrence to equation (4). Also from this example, there now appears to be a means to generalize the results derived so far. First it is useful to cast the dynamics of

equation (3) into the framework as a nonlinear filter processing a scalar input signal *S(t)* with an additive noise disturbance $\xi(t)$.

5. A NONLINEAR FILTER RELATIONSHIP TO DESCRIBE THE SR EFFECT

In Fig. 4, is displayed a filter representation of the input-output parameters of equation (3). The nonlinear function

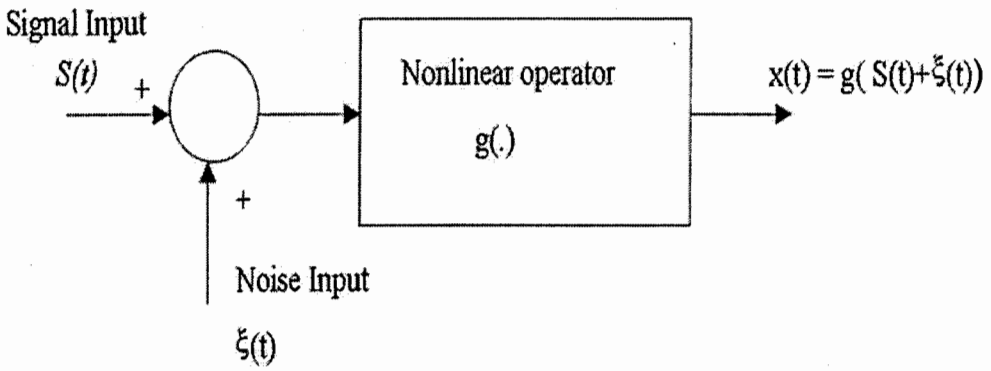

Fig. 4 – A filter perspective on the SR effect

$g(S(t)+\xi(t))$ represents the right hand side of equation (3). In this context the SR effect results from a nonlinear filter and the goal is to see what value can be gained from this representation. A wider class of such filters is now discussed.

6. GENERALIZATION OF SR TO OTHER MATHEMATICAL PARADIGMS

It was shown in section 5 that a relationship exists between the physical example and its equilibrium points within a mathematical framework. This can easily be extended to a wider class of systems (Ref. 28) as follows: Consider a class of filters, such as in Fig. 4, with the following principle property (e.g. for state variables $\dot{x}_1 = x_2$):

Property 1: In the region of the state space $x_{1a} \leq x_1 \leq x_{1b}$ the equilibrium points along the x_1 axis have the following characteristics: two stable equilibrium points are interlaced between one unstable equilibrium point.

In Fig. 4, the SR effect will occur (at least locally) in the region $x_{1a} \leq x_1 \leq x_{1b}$ which may not be global, but sufficient to have applicability. Fig. 5 shows such a rendering. Some simple examples of g(.) are listed (Ref. 28):

Example 1: $g(.) = \dot{x} = -(x+a_1)(x+a_2)(x-a_3)(x-a_4)(x-a_5)$, with $a_5>a_4>a_3>a_2>a_1$ and for all $x < a_4$. (5)

Example 2: $g(.) = \dot{x} = (x+a_1)(x+a_2)(x+a_3)(x-a_4)(x-a_5)(x-a_6)(x-a_7) + (a_8)(e^{-b_1 x} - e^{-b_2 x}) + (a_9)(e^{-b_3 x} - e^{-b_4 x})$, (6)

$a_7>a_6>a_5>a_4>a_4>a_3>a_2>a_1$, $b_i>0$ and the SR effect occurs for all values of x. A number of other such functions can also be synthesized. In both examples above, the potential energy function *V(x)* is ***shaped*** (cf. Fig. 5) to produce physical equilibrium points analogous to Fig. 3 in the region of interest. This induces an SR effect, at least locally near the areas where the interlacing of an unstable equilibrium point between two stable equilibriums is achieved. Thus, by designing the filter through manipulation of equilibrium points, different filter dynamics can be achieved. We first describe tests on the efficacy of the method for a simple signal processing example to examine the signal to noise amplification gains that can be achieved.

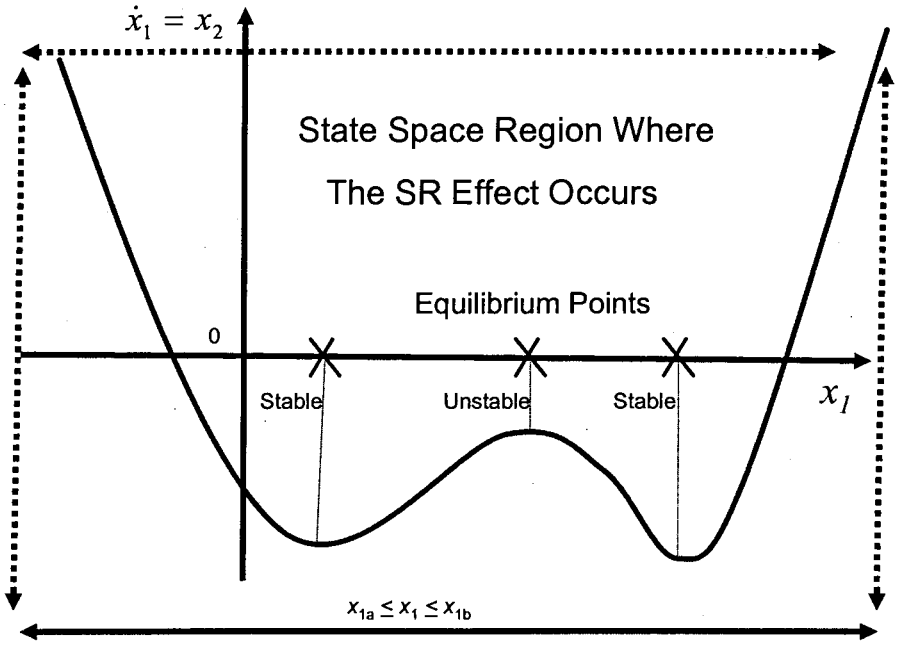

Fig. 5 – State space region where the SR effect occurs

7. TEST CASE-1 A SIGNAL PROCESSING EXAMPLE

The first example considered will evaluate the efficacy of the SR method to amplify signal-to-noise ratio using scalar signals. The literature abounds on related examples (Ref. 9-13). For this test, $S(t)$ is selected to be the sum of two unity amplitude sinusoids at frequencies of 1 and 4 hertz, respectively. The noise term $\xi(t)$ is chosen to be zero mean Gaussian with variance ($gain_2$) which will be increased from zero. The input signal to noise ratio in Fig. 4 is determined on the left from the signals $S(t)$ and $\xi(t)$ through Fourier transform estimates of these signals. The combined signal is then passed through the SR filter in Fig. 4. At the output of that filter, to the right, yields the output signal-to-noise ratio which is evaluated by performing a FFT (Fast Fourier Transform) on the output $x(t)$ and comparing this signal power at the two frequencies (1 and 4 Hz) to the adjacent frequency bins. Thus using the calculated input SNR (signal to noise ratio) and derived output SNR, the SNR ratio gain amplification is then determined via:

$$\text{Gain Amplification of SNR through the SR filter} = \text{(Output SNR) / (Input SNR)} \tag{7}$$

The dynamics of the SR filter for this test case were selected to satisfy equation (3) for the case $a = 1$. Fig. 6 shows the time series for $S(t)$ in real time and Fig. 7 is the corresponding FFT for a low level of signal plus noise ($S(t)+\xi(t)$). Herein it can be seen that the dominant spectral content of $S(t)$ occurs at 1 and 4 Hz is obvious. Fig. 8 shows the spectral output of the SR filter ($x(t)$) for a very high level of noise. The $1/f$ effect on the signals seems clear so the second component of $S(t)$ at 4 Hz is less pronounced. The SNR calculation can still be conducted. Fig. 9 demonstrates the SNR gain as a function of the intensity of the independent noise variable ($gain_2$). The upper plot in Fig. 9 is the SNR from the output of the SR filter. The lower plot is what the SNR would have been in the absence of the SR filter. The difference between the end points (SNR gain from the SR filter) of the curves is greater than a 10^6 amplification and appears to have no limit, even though this is a contrived example. Figure 10 shows the computational cost to achieve these calculations. It is seen that the computational complexity is exponential (NP-hard) due to the need to perform the numerical integration and error convergence using 4th order -Newton-Raphson-Runge-Kutta via the MATLAB™ function "ode45" for stiff differential equations. Figure 11 displays the real time output of the SR filter via ($x(t)$ and

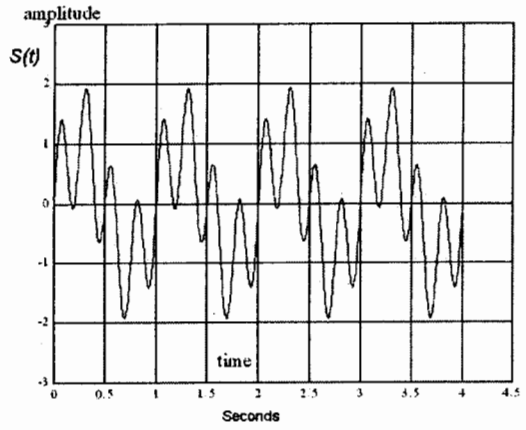

Fig. 6 – The deterministic function $S(t)$ in real time

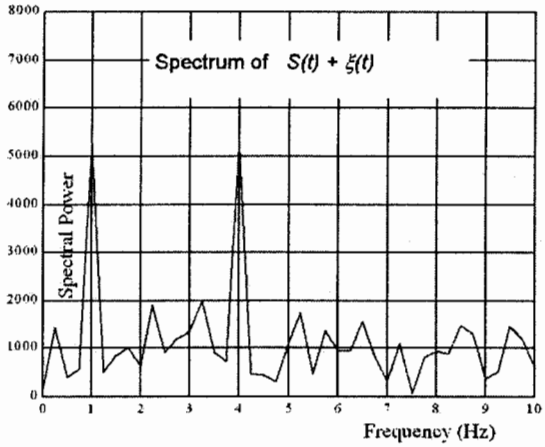

Fig. 7 – Spectrum of $S(t) + \xi(t)$ for low level noise

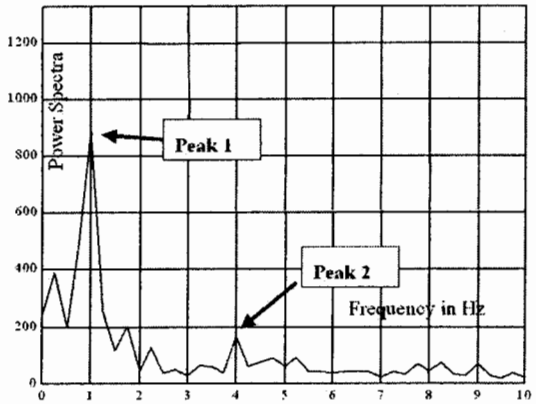

Fig. 8 – Spectrum of $x(t)$ for high level noise

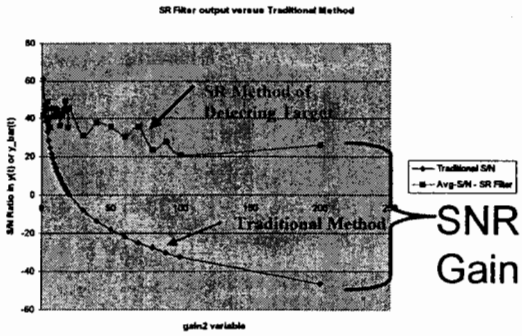

Fig. 9 – SNR Amplification gain versus noise power

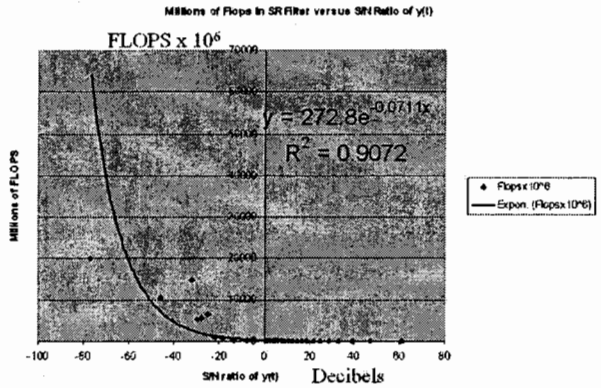

Fig. 10 – Computation cost for numerical integration

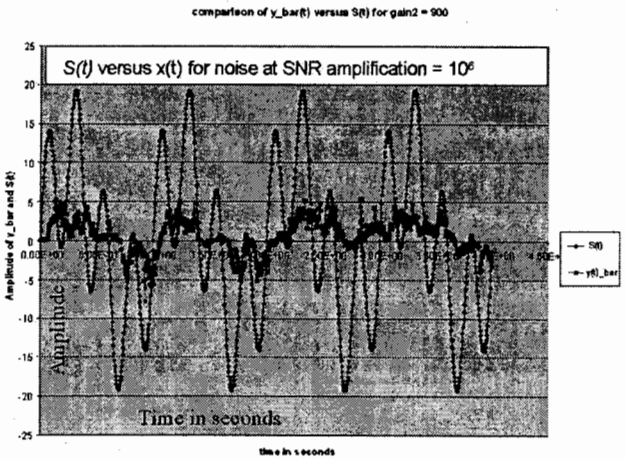

Fig. 11– $S(t)$ versus $x(t)$ for worst case noise

$S(t)$) for the worst case noise used in these simulations. This method is now applied to the object recognition problem involving images.

8. TEST CASE 2- AN IMAGE RECOGNITION PROBLEM

Fig. 12a portrays object 1 and Fig. 12b displays object 2. The goal is to distinguish these objects inside test images which may be compromised. A comparison of the respective intensity histograms are displayed in Fig. 13. The distinction of the two objects will be based on a method employing intensity histograms (Ref. 29) using a SR approach.

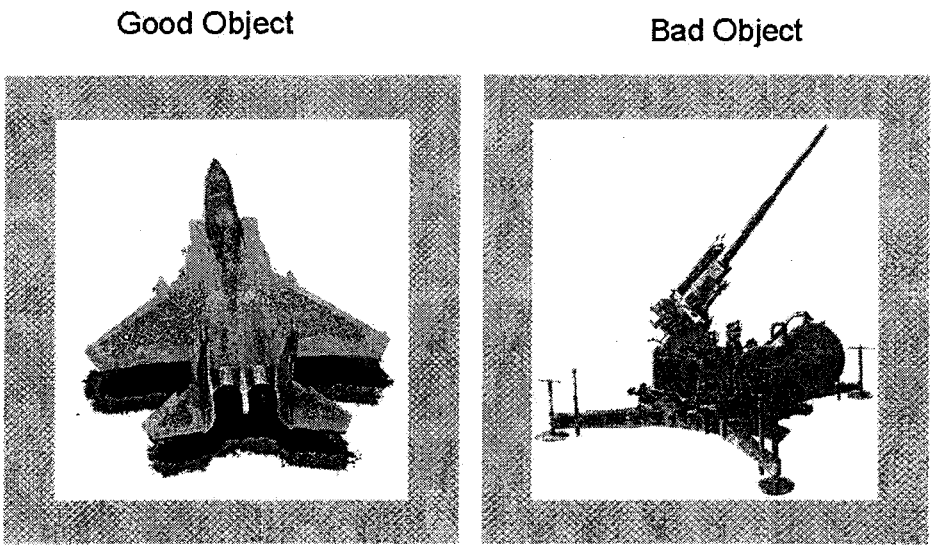

The Good Object versus the Bad Object for the Identification Problem of Interest

Fig. 12a – The good object (F-15A aircraft) Fig. 12b – The bad object (anti-aircraft gun)

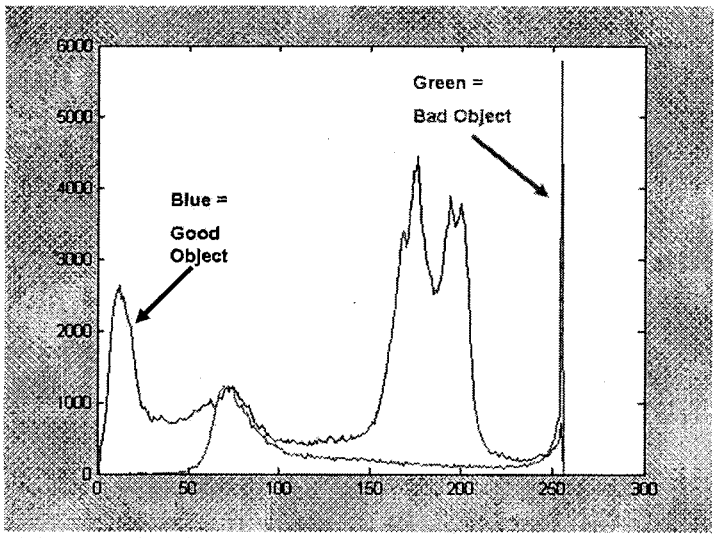

Histogram Signatures of the Good Object versus the Bad Object.

Fig. 13 – Histogram signatures of good versus bad object from Figs. 12a-b

It is noted that the sample images in Figs. 12a-b were derived from web-based sources freely available to the public and do not constitute any specific military information. The development of the SR process proceeds in six steps;
Step 1: A test image is scanned for a possible friendly or hostile object.
Step 2: A sample image from the test image is compared to possible library templates for friendly or hostile objects.
Step 3: A distance norm determines a relative separation between the sample and each library object.
Step 4: A perturbation is then made in the requisite histogram signatures and steps 2-4 are repeated.
Step 5: Votes are developed based on low values of the norm distance from the sample to particular library objects.
Step 6: The threshold operation is synthesized by a majority voting scheme of the constituent voters.
A standard to fairly compare the efficacy of different image identification algorithms is now described.

9. A TEST TO COMPARE ALGORITHMS FOR OBJECT RECOGNITION IN IMAGES

Fig. 14 displays a possible means of objectively comparing and quantifying the efficacy of different algorithms in this object identification problem. For this paper, three major factors that influence the ability to discern objects in images include image contrast, brightness (amount of light being transmitted back to the observer from the image), and relative size of the key objects. The good and bad objects in Fig 12a-b at normal size, contrast, and intensity are calibrated and appear at the origin in Fig. 14. The three axes show various levels of degradation away from the origin in the directions of decreasing contrast, changing brightness, and reduction in size. The point in which an algorithm fails (defined e.g. less than 60% correct detection in a binary detection task) may define the limit of performance of the algorithm. Thus the distance from the failure point to the origin in Fig 14 is a possible measure to objectively state the efficacy of an object identification algorithm. Hence algorithms can be compared one against the other for their relative efficacy.

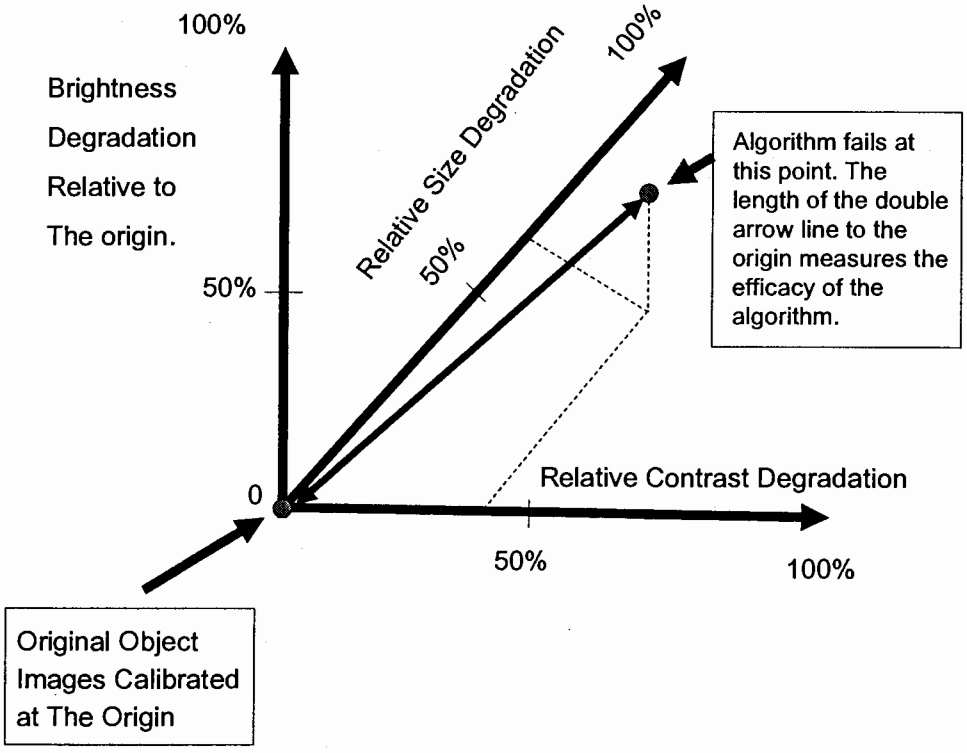

Fig. 14 – Standard to compare object identification algorithms in images

10. RESULTS OF THE SR IMAGE RECOGNITION SYSTEM

Similar to a procedure as discussed in Ref. 30, the approach to using an SR technique to improve the detection of objects in images will consist of two principal steps:
Step 1: Provide some perturbation in the original data set or analysis method.
Step 2: Threshold the effect in a manner to make decisions on the identity of the object.
It is noted the analogy to the biological system displayed in Fig 1 is very intentional and the goal here is to use a "bioinspired" methodology to see the benefits that may be gleaned from such a process.

Since it is easier to describe Step 2 first, the thresholding method is discussed next.

10.1 The means of implementing the threshold action

In a companion paper (Ref. 31) the two library objects in Figs. 12a-b were used as a basis for object identification. A sample image had white Gaussian noise added of increasing intensity to a library image. The goal was to discern the ground truth (which of the two objects were in the sample image) as the noise power increased. The efficacy of the algorithm was determined via the ability to correctly distinguish the two images in this Monte Carlo simulation. As the noise intensity increased, four measures or a metric were selected to correctly discern the two possible objects. To produce the threshold action, a majority voting scheme would select the bad object if the number of votes was greater than or equal to the majority. This scheme would choose the good object if the majority vote was less than 2.5 votes. The thresholding was implemented as shown in Fig 15.

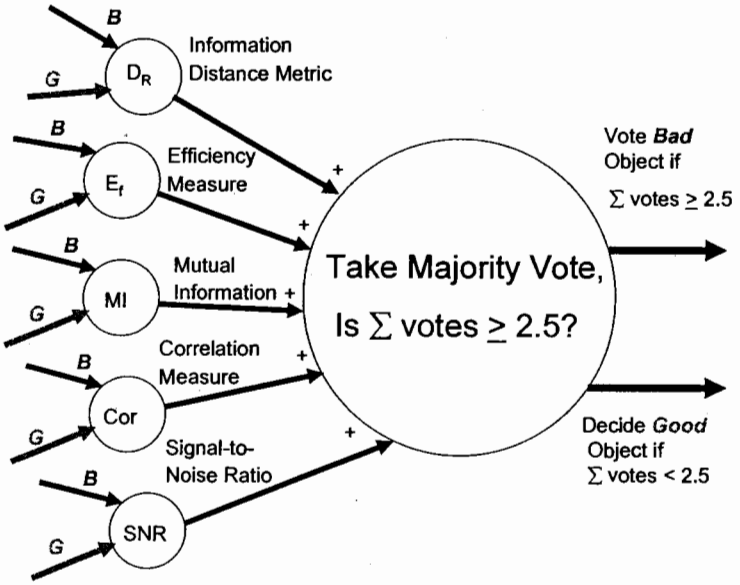

Fig. 15 – Majority voting scheme as the requisite threshold operator

The five measures/metric in Fig 15. are described in greater detail in Ref. 31. Finally a performance comparison between the two cases: Case 1 (no SR effect) versus Case 2 (SR method implemented) are presented next.

10.2 Results of two cases of Monte Carlo simulation

The two cases of interest are described from their Monte Carlo simulation. Case 1 is the performance of the system as portrayed in Fig 16. without the SR effect implemented in the algorithm. Case 2 (Fig. 17) shows the similar system (all other parameters are the same) but with the SR method in operation. The ground truth is the friendly object so the

correct decision would have the sum of all the majority votes ≤ 2.5. The performance of the algorithm in Fig, 16 can be quantified by looking at the ground truth condition (good object) as the noise intensity increases (no SR effect). The algorithm eventually fails when the majority vote approaches the chance condition of 2.5 votes. The level of the noise intensity can be measured off the x-axis in Fig. 16 before the confusion occurs. For Case 2 conditions, Fig 17. portrays a similar Monte Carlo demonstration when the SR effect is implemented in the simulation. All other parameters in the simulation are the same.

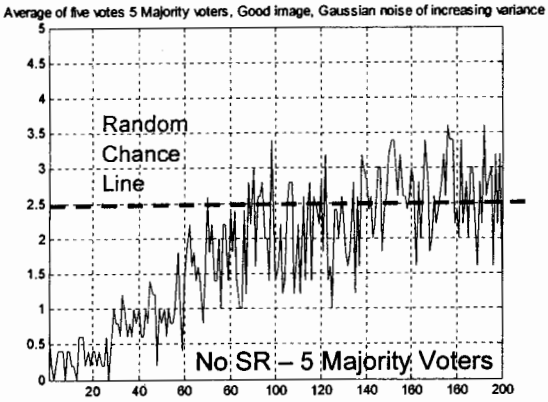

Fig. 16 – Case 1 – Good image without SR - noise increasing

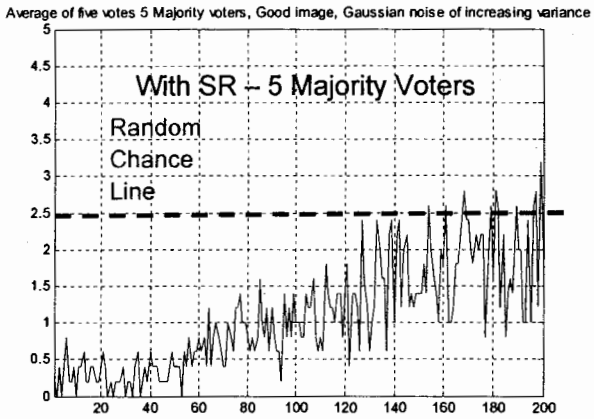

Fig. 17. – Case 2 – Good image with SR – noise increasing

11. CONCLUSIONS

Contrasting Figs. 16 to Fig. 17 it is seen that the SR implementation into the majority voting scheme allows the algorithm to perform more correctly (closer to the ground truth) with the SR effect in operation for higher values of noise intensity being added into the image. One method to effectively compare algorithms is to take the point where the detectors fail to correctly distinguish the ground truth. From Figs 16-17, there is over a 100% improvement in performance using the SR method as compared to traditional detection methods as measured by the level of noise intensity before the ground truth becomes confused with the hostile object.

REFERENCES

1. R. Benzi, A. Sutera, and A. Vulpiani, "The mechanism of stochastic resonance," *J. Phys.*, **vol A14**, pp. L453-457, 1981.
2. J. J. Collins, C. C. Chow, and T. T. Imhoff, "Aperiodic stochastic resonance in excitable systems," *Physical Review E*, **vol. 42** (4), October, 1995, pp. R3321-R3324.
3. B. Kosko and S. Mitaim, "Stochastic resonance in noisy threshold neurons," *Neural Networks*, **vol. 16**, 2003, pp. 755-761.
4. J. D. Harry, J. B. Niemi, A. A. Priplata, and J. J. Collins, "Balancing Act – Noise is the key to restoring the body's sense of equilibrium, " *IEEE Spectrum*, pp. 37-41, April, 2005.
5. D.W. Repperger, C. A. Phillips, J. E. Berlin, A. T. Neidhard-Doll, and M. W. Haas, "Human-Machine Haptic Interface Design Using Stochastic Resonance Methods," *IEEE Trans. on Systems, Man, and Cybernetics –Part A: Systems and Humans,* **vol. 35** (4), July, 2005, pp. 574-582.
6. P. Harmer, B. R. Davis, and D. Abbott, "A Review of Stochastic Resonance: Circuits and Measurement," *IEEE Trans. On Instrumentation and Measurement*, **vol. 51** (2), April, 2002, pp. 299-309.
7. S. Zozor and P-O Amblard, "Stochastic Resonance in Locally Optimal Detectors," *IEEE Trans. on Signal Processing*, **vol. 51**, (12), December, 2003, pp. 3177-3181.
8. S. Kay, "Can Detectability be Improved by Adding Noise," *IEEE Signal Processing Letters*, **vol. 7**, (1), January, 2000, pp. 8-10.

9. P. Makra, Z. Gingl, and L. B. Kish, "Signal-to-noise ratio gain in non-dynamical and dynamical bistable stochastic resonators," *Fluctuation and Noise Letters*, **vol. 2**, pp. L147-L155, 2002.
10. G. Liu, Y. Yu, and W. Wang, "Signal-to-noise ratio gain in neuronal systems," *Physical Review E*, **vol. 63**, 2001.
11. F. Chapeau-Blondeau, "Periodic and aperiodic stochastic resonance with output signal-to-noise ratio exceeding that at the Input," *International Journal of Bifurcation and Chaos*, **9**, pp. 267-272, 1999. vol. 232, pp. 41-48, 1997.
12. F. Chapeau-Blondeau, "Input-Output gains for signal in noise in stochastic resonance," *Physics Letters A*, **vol. 232,** pp. 41-48, 1997.
13. K. Loerincz, Z. Gingl, and L. B. Kiss, "A Stochastic Resonator is Able to Greatly Improve Signal-to-noise Ratio," *Physics Letters A*, **vol. 2224**, (1996), pp. 63-67.
14. C. Heneghan, C. C. Chow, J. J. Collins, T. T. Imhoff, S. B. Lowen, and M. C. Teich, "Information measures quantifying aperiodic stochastic resonace," *Physical Review E*, **vol. 54** (3), September, 1996, pp. R2228-R2231.
15. A. R. Bulsara and A. Zador, "Threshold detection of wideband signals: A noise-induced maximum in the mutual information," *Physical Review E*, **vol. 54** (3), September, 1996, pp. R2185-R2188.
16. M. E. Inchiosa, J. W. C. Robinson, and A. R. Bulsara, "Information-theoretic stochastic resonance in noise-floor limited systems: The case for adding noise," *Phy. Rev. Lett.*, **vol. 85**, pp. 3369-3372, Oct. 2000.
17. D. R. Carreta Dominguez and E. Korutcheva, "Three-state neural network: From mutual information to the Hamiltonian," *Physical Review E*, **vol. 62**, (2), August, 2000, pp. 2620-2628.
18. L. B. Kish, G. P. Harmer and D. Abbott, "Information transfer rate of neurons: stochastic resonance of Shannon's information channel capacity," *Fluctuation and Noise Letters*, **vol. 1**, (1), 2001, pp. L13-L19.
19. P. Viola and W. M. Wells, "Alignment by Maximization of Mutual Information," *International Journal of Computer Vision*, **vol. 24** (2), 1997, pp. 137-154.
20. S. Mitaim and B. Kosko, "Adaptive Stochastic Resonance in Noisy Neurons Based on Mutual Information," *IEEE. Trans. on Neural Networks*, **vol. 15**, (6), November, 2004, pp. 1526-1540.
21. M-O Hongler, Y. L. de Meneses, A. Beyeler, and J. Jacot, "The Resonant Retina: Exploiting Vibration Noise to Optimally Detect Edges in an Image," *IEEE Trans. on Pattern Analysis and Machine Intelligence*, **vol. 25**, (9), September, 2003, pp. 1051-1062.
22. Goychuk and P. Hanggi, "Stochastic Resonance in Ion Channels Characterized by Information Theory," *Physical Review E*, **vol. 61**, (4), April 2000, pp.4272-4280.
23. F. Vaudelle, J. Gazengel, and G. Rivoire, "Stochastic resonance and noise-enhanced transmission of spatial signals in optics: the case of scattering," *J. Opt. Soc. Am. B,* **vol. 15** (11), November, 1998, pp. 2674-2680.
24. S. Mitaim and B. Kosko, "Adaptive Stochastic Resonance," *Proceedings of the IEEE*, **vol. 86**, (11), November, 1998, pp. 2152-2183.
25. H-P Muller, E. Kraft, A. Ludolph, and S. N. Erne, "New Methods in fMRI Analysis," *IEEE Engineering in Medicine and Biology*, September/October, 2002, pp. 134-142.
26. X. Wu, Z-P Jiang, D. W. Repperger, and Y. Guo, "Enhancement of Stochastic Resonance Using Optimization Theory," *Communications in Information and Systems*, **vol. 6**, No. 1, 2006, pp. 19-36.
27. N. G. Stocks, "Suprathreshold Stochastic Resonance in Multilevel Threshold Systems," *Physical Review Letters*, **vol. 84**, (11), 13 March, 2000, pp. 2310-2313.
28. D. W. Repperger, M. S. Djouadi, et. al., US patent #7,030,808 B1– "Nonlinear Target Recognition," 04/18/06.
29. J. C. Russ, *The Image Processing Handbook*, Fourth Edition," CRC Press, 2002.
30. C. D. Schrider, J. A. Skipper, D. W. Repperger, "Histogram-based Template Matching for Object Detection in Images with Varying Contrast," *Proceedings of the IS&T / SPIE's XIX Annual Symposium on Electronic Imaging*, 2007, San Jose, California, USA.
31. D. W. Repperger, A. R. Pinkus, J. A. Skipper, C. D. Schrider, "Object recognition via information-theoretic measures/metrics ," *Proceedings of the IS&T / SPIE's XIX Annual Symposium on Electronic Imaging*, 2007, San Jose, California, USA.